Integrated Ultra-Low-Loss Silicon Nitride Waveguide Coil for Optical Gyroscopes

Sarat Gundavarapu[*], **Taran Huffman**[*], **Renan Moreira, Michael Belt, John E. Bowers and Daniel J. Blumenthal**

Department of Electrical and Computer Engineering, University of California, Santa Barbara, CA 93106, U.S.A
saratchandra@ece.ucsb.edu
* These authors contributed equally to this project

Abstract: We demonstrate, for the first time, a Sagnac sensor using an on-chip 3m ultra-low-loss silicon nitride waveguide coil.
OCIS codes: (060.2800) Gyroscopes; (280.4788) Optical sensing and sensors; (130.6010) Sensors; (060.2370) Fiber optics sensors; (230.7390) Waveguides, planar; (130.3120) Integrated optics devices;

1. Introduction

High sensitivity optical gyroscopes have a wide variety of applications including guiding ballistic missiles, navigating air-crafts, autonomously controlling underwater vehicles, and geographic surveying [1]. Considerable amount of research has gone in to the characterization and miniaturization of interferometric optical gyroscopes (IOG), while maintaining high performance. A significant engineering challenge exists here, as the sensitivity of an IOG improves with the length and area of the coil. Our Si_3N_4 based ultra-low loss (ULL) waveguide platform [2] provides a solution to overcome these challenges and create an integrated millimeter scale device.

In this paper, we demonstrate, to the best of our knowledge, the first on-chip integrated coil for an IOG on an ULL high aspect ratio Si_3N_4/SiO_2 planar waveguide platform. The Sagnac effect is demonstrated using a 3m on-chip waveguide coil in tandem with fiber based components. The results are compared with a fiber only gyroscope.

2. Design and Fabrication

Waveguide width and thickness are the primary parameters in determining waveguide loss, bend limitations, and crossing loss [2]. The waveguide schematic is shown in Fig. 1 (a), where w=5μm and t1=60nm. Fabrication begins on a 0.5mm thick, 100mm diameter silicon substrate, upon which 15μm of thermal SiO_2 is grown. The core Si_3N_4 layer is deposited using low pressure chemical vapor deposition (LPCVD). The core is defined with a single lithographic step and dry etch, designed for vertical sidewalls and low sidewall roughness. The upper SiO_2 cladding is deposited using reactive co-sputtering, with t2=3μm. Further details can be found in [2]. Because two inputs are required, the coil is a spiral with a tight inner bend, near the bend limit of the waveguide geometry. The waveguide then crosses the spiral for the second input, shown in Fig. 1 (b). In this figure R1=7.5mm, R2=3mm, and there are 90 crossings.
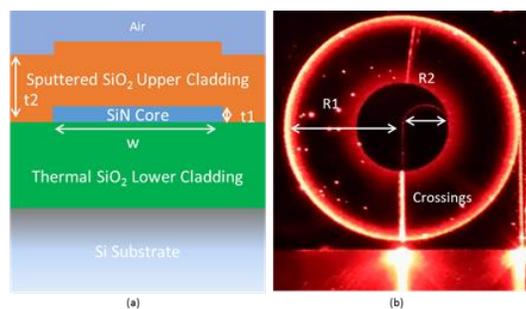

Fig, 1. (a) Cross-section schematic of the waveguide design. (b) Top-down schematic of waveguide coil

3. Coil characterization

The crossing loss was measured using multiple structures to simulate the cut-back method. Each facet was coupled to using 2μm lensed fibers. Across two die, linear fits result in a crossing loss of 0.039 dB/crossing, with R^2=0.963 and R^2=0.945, as shown in Fig.2 (a). The total crossing loss penalty is therefore approximately 7 dB.
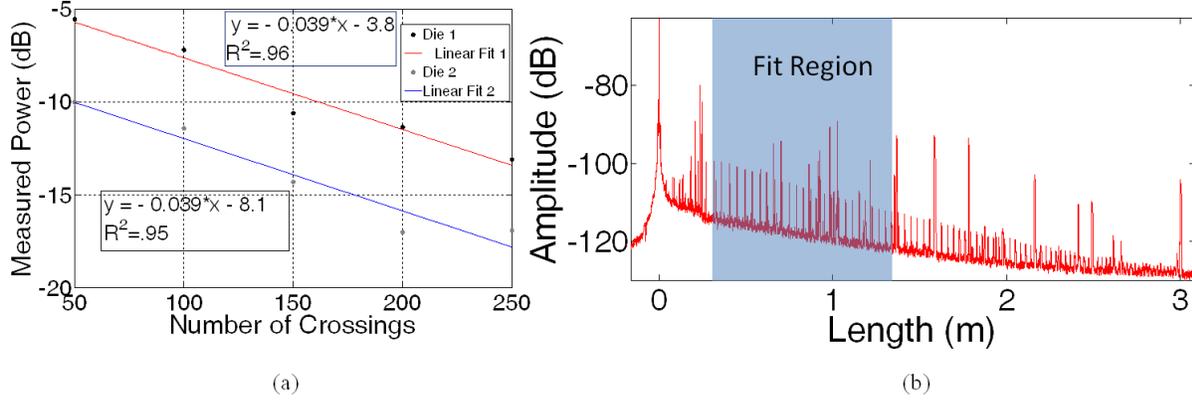
Fig, 2. (a)Crossing loss cutback fit. (b) OBR trace and fit.

The waveguide loss was measured using an optical backscatter reflectometer as in [2]. Looking at the trace in Fig. 2 (b), we can clearly see the reflections from the waveguide crossings in the coil. In addition, the trace presented possesses some other scattering centers from defects. However, we can fit a slope, 1.45m long (highlighted in the fit region), to areas outside of excess scatterers, which yields a loss of 3.3 dB/m. We can remove the crossing losses contributing to that value, which marginally improves the result to 2.5 dB/m. This gives a total theoretical penalty, outside of additional scatterers and coupling losses, of 14.4 dB.

4. Gyro Measurements

The output power of IOG is a sinusoidal function given by (1) where $\Delta\Phi_R$ is the induced phase shift, $\Phi_m(t)$ is the applied modulation, $\Delta\tau_g$ is the group transit time and $\Delta\Phi_m(t)$ is the phase difference between the counter propagating waves due to applied modulation. For a coil with effective refractive index n_{eff}, effective diameter D_{eff}, and a light source of mean wavelength λ, a phase shift of $\Delta\Phi_R$ can be induced by applying a rotation rate Ω as given in (3) or by using sawtooth/serrodyne modulation of frequency, f_R as given in (4) [3,4]. The effective length of a gyro coil, L_{eff} is the path difference between the long and short paths that connect the modulator and splitter. Note that $L_{eff} \approx L_{fiber}$ for longer coils that are generally used in fiber optic gyros, but this distinction is important as we move towards shorter on-chip coils, where even the length of the pigtails of components can be a significant percentage of the total length of the coil.

$$P(\Delta\Phi_R) = P_0[1+cos(\Delta\Phi_R + \Delta\Phi_m(t))] \tag{1}$$

$$\Delta\Phi_m(t) = \Phi_m(t) - \Phi_m(t-\Delta\tau_g) \tag{2}$$

$$\Delta\Phi_R = 2\pi\cdot\left(\frac{\Omega \cdot D_{eff}}{n_{eff}\lambda}\right)\cdot\Delta\tau_g \tag{3}$$

$$\Delta\Phi_R = 2\pi\cdot f_R\cdot\Delta\tau_g \tag{4}$$

$$\Delta\tau_g = \left(\frac{n_{eff}\cdot L_{eff}}{c}\right); \quad f_p = \left(\frac{1}{2\Delta\tau_g}\right) \tag{5}$$

To operate at maximum sensitivity, a square wave modulation, $\Phi_m(t) = \mp\left(\frac{\pi}{4}\right)$ rad is applied to the phase modulator, which results in $\Delta\Phi_m(t) = \left(\frac{\pi}{2}\right)$ rad. If the frequency of the modulation is set to f_p, as given in (5), the odd harmonics of f_p in the gyro output intensity are minimized and the phase modulation will not affect the minimum detectable rate [5].

The proper frequency of the coil, f_p was measured using a linear frequency sweep of the sawtooth signal, applied to the phase modulator as shown in Fig. 4 (a). The setup is similar to a closed loop configuration of fiber optic gyro using serrodyne modulation [3]. Here, the sawtooth function generator was also used to generate a reference signal for the lock-in (as indicated using the dotted lines in Fig. 4 (a)). The square wave and trigger generators were left off for this measurement. The fly back time of the sawtooth wave was kept very small and the reset amplitude was set to 2π radians to minimize errors. The (fiber + on-chip) coil configuration was tested and compared to a nearly equal length fiber only version of the gyro. Additional attenuators (not shown in the figure) were added in the fiber only version of the gyro to match with the system losses of the on-chip coil. The results of the proper frequency sweep, along with the corresponding effective length (calculated using (5) with $n_{eff}= 1.5$) are shown in Fig. 5 and are in good agreement with the actual coil lengths.

To measure the rotation signal using gyro, the square wave generator in Fig. 4 (a) was adjusted to switch between $\mp\left(\frac{\pi}{4}\right)$ rad and was synced with the sawtooth waveform using a 300 MHz trigger generator. The square wave output was also used as a reference signal for the lock-in. A rotation signal measurement of the fiber only gyro version, was taken using a 1270VS Ideal Aerosmith stage, with an applied rotation rate varying from 0.02 °/sec to 5 °/sec, as shown in Fig. 6(a)(the sawtooth generator was turned off during this measurement) . Scale factor of the gyro was calculated from this data, using a linear fit, to be $0.6\left(\frac{\mu V}{^\circ/\text{sec}}\right)\mp 0.36\mu V$. The sawtooth frequencies were then calibrated for the fiber only and (fiber + on-chip coil) configurations of the gyro to match with the output voltage values from the physical rotation measurement, as shown in Fig. 6(b) (For small rotation rates, identical voltage values on the lock-in at f_p, indicate equal induced phase shift.). From (3),(4), and (5), the sawtooth frequency input, f_R, required to produce the same induced phase shift as the rotation rate input, Ω, for the same light source, depends on the dimensions of the coil ($L_{eff}\times D_{eff}$). This value is directly related to the scale factor of the gyro and can be calculated from the slope of the curves in Fig. 6(b), which are $2.3\left(\frac{KHz}{^\circ/\text{sec}}\right)\mp 2.8KHz$ for the fiber only configuration and $5.3\left(\frac{KHz}{^\circ/\text{sec}}\right)\mp 3.6KHz$ for the (fiber + on-chip coil) version. In other words, the scale factor of (fiber + on-chip coil) is about $0.3\left(\frac{\mu V}{^\circ/\text{sec}}\right)$ (nearly half of the fiber only configuration).
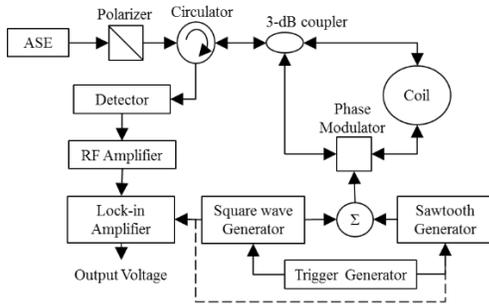

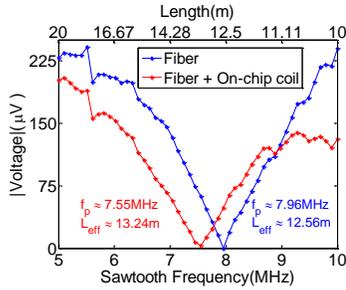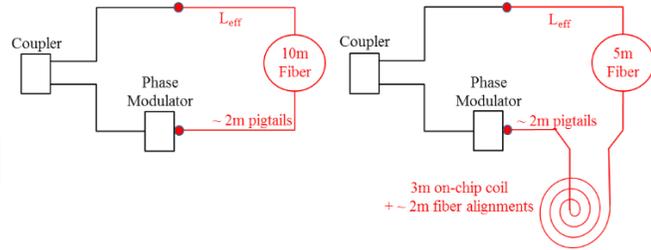Fig. 4(a). Schematic of IOG measurement setup   Fig. 4(b). Coil Setups – Fiber Only and (Fiber + 3m On-chip)
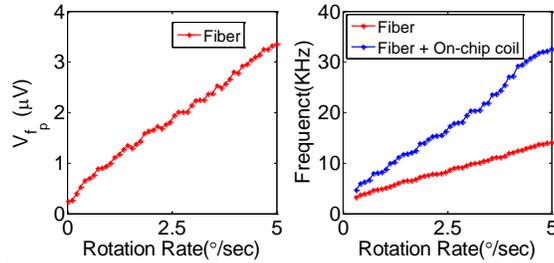

Fig. 5. Proper Frequency Measurement   Fig. 6. (a) Rotation signal measurement (b) Equivalent sawtooth frequencies

4. Conclusion

We demonstrated, for the first time, a Sagnac sensor using an on-chip 3m ULL Si_3N_4 waveguide coil. We reported a new way of calibrating the proper frequency of an IOG using the frequency sweep of a serrodyne modulation. Directions for the future include: reducing scatterers, packaging the coil to significantly reduce the losses, and implementing digital closed loop control to improve the gyro's performance.

5. References

[1] Lutwak, R., "Micro-technology for positioning, navigation, and timing towards PNT everywhere and always," in *Inertial Sensors and Systems (ISISS), 2014 International Symposium on* , vol., no., pp.1-4, 25-26 Feb. 2014
[2] Jared F Baters, "Ultra-low-loss high-aspect-ratio Si_3N_4 waveguides", Opt. Express 19,Issue 4, page 3163-1374, 2011
[3] Herve C. Lefevre, "The Fiber-Optic Gyroscope"
[4] Zhonghe Jin, Xuhui Yu, and Huilian Ma, "Closed-loop resonant fiber optic gyro with an improved digital serrodyne modulation," Opt. Express 21, 26578-26588 (2013)
[5] R. A. Bergh, H. C. Lefevre, and H. J. Shaw, "All-single-mode fiber-optic gyroscope with long-term stability," Opt. Lett. 6, 502-504 (1981)